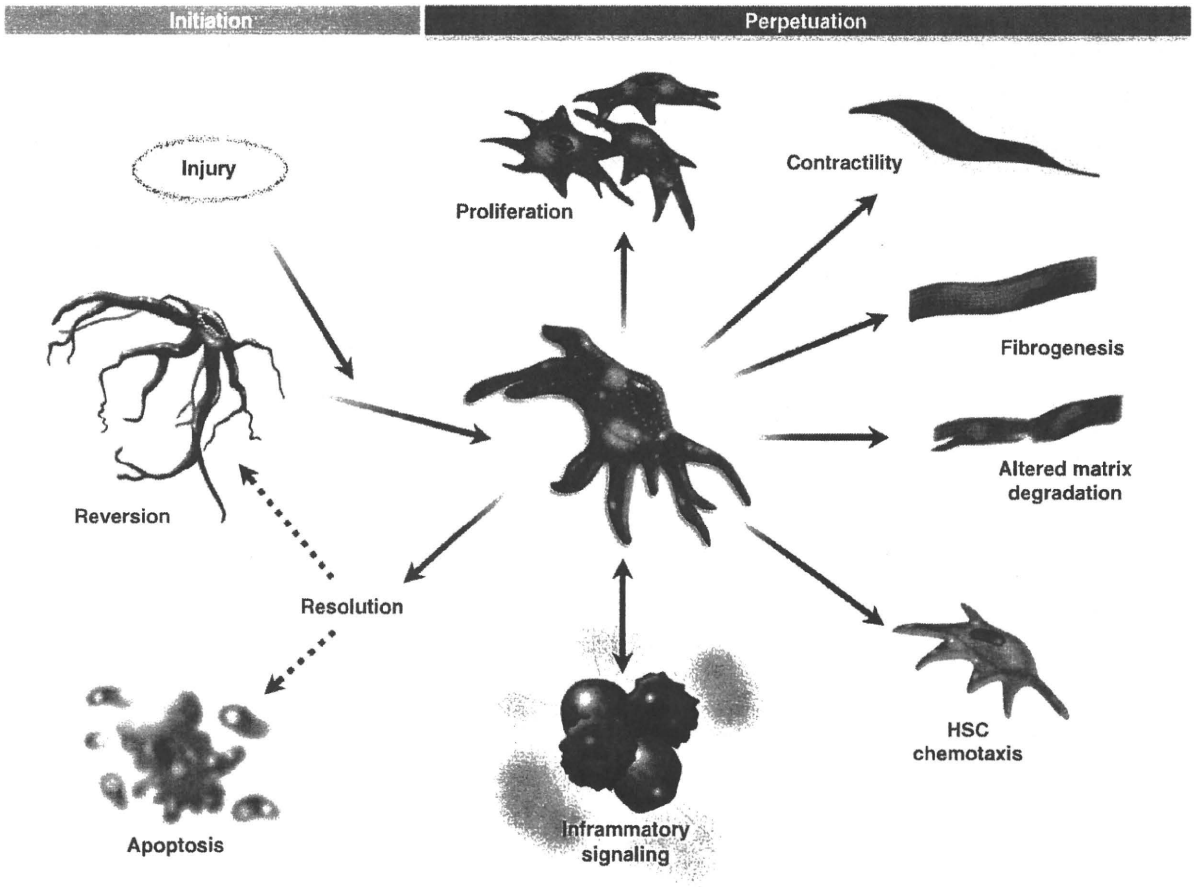

Figure 2 Illustrative demonstration of activation and deactivation of stellate cell and the related cellular function. When liver injury takes place, stellate cells undergo activation and switch their phenotype from a vitamin A-storing one to myofibroblast-like one that expresses α-smooth muscle actin. The latter phenotype of stellate cells proliferate, have contractile activity and produce extracellular matrices including type I collagen, inhibitors of matrix metalloproteinases and pro-inflammatory mediators. In addition, they acquire chemotactic activity. In the resolution stage of liver fibrosis, activated stellate cells undergo either apoptosis or reversion to the original vitamin A-storing phenotype.

Perpetuation of fibrotic response in the liver

Perpetuation of the hepatic fibrotic process is supported by the activation of HSC and the presence of MFB, which are continuously stimulated by growth factors, cytokines and oxidative stress, which are derived from neighboring cells. Damaged hepatocytes are a source of lipid peroxides and reactive oxygen species (ROS) generated from hepatocytic mitochondria, and breakdown products of the hepatocyte membrane activate HSC.[17] Nicotinamide adenine dinucleotide phosphate oxidase is an important component of the ROS-producing system, which could be a target for antifibrotic therapy. This enzyme is supposed to be induced in HSC to dispose of cells undergoing apoptosis, and lowering its expression in HSC by rosaltan, an angiotensin receptor antagonist, results in the decreased production of type I collagen and matrix metalloproteinase (MMP)-2.[18] Alternatively, excess accumulation of Fe^{2+} triggers the Fenton reaction to generate a radical·OH and leads to the apoptosis of hepatocytes, resulting in the activation of HSC and promotion of the fibrotic process.

Transforming growth factor-α, TGF-β, insulin-like growth factor and its binding protein, hepatocyte growth factor (HGF), VEGF and interleukin (IL)-6 are supposed to be candidates released from hepatocytes to

trigger HSC activation. On the other hand, when liver injury takes place, Kupffer cells become activated by oxidative stress and endotoxin lipopolysaccharide (LPS) derived from intestinal flora through Toll-like receptor (TLR)4 and CD14.[19] Macrophage chemotactic protein-1 (MCP-1) and osteopontin derived from activated Kupffer cells are involved in the infiltration of inflammatory cells into the liver.[20] In addition, activated Kupffer cells generate PDGF and TGF-β1, which in turn induce HSC activation. In an animal model, depletion of Kuppfer cells using the administration of gadolinium chloride ameliorates hepatic fibrosis, suggesting the active participation of Kupffer cells in hepatic fibrogenesis. Functional roles of chemokines in liver injury and fibrotic process are also discussed.[21]

Recent investigations revealed that, in addition to macrophages, Kupffer cells and classical lymphocytes (T and B cells), natural killer (NK) cells, NKT cells, dendritic cells and mast cells are important players in liver fibrosis, whose cellular functions are regulated by the TLR system and NF-κB signaling pathways. Namely, interaction between HSC/MFB and these immune-regulatory cells take part in the local infiltration of inflammatory cells in hepatic sinusoids.[22]

It was noted that cannabinoid receptors and their endogenous ligands are new players in liver fibrosis and in the activation process of HSC.[23] Three major components of cannnabinoids are tetrahydrocannabinol, cannabinol and cannabidiol whose receptors are composed of CB1 and CB2. Hemp and marijuana accelerate fibrosis progression in chronic hepatitis C and cannabinoids are also assumed to be associated with non-alcoholic steatohepatitis because CB1 receptor antagonists suppress appetite. HSC express both CB1 and CB2. The CB2-dependent signal initiates the apoptosis of HSC, CB1 level increases depending on HSC activation and regulation of its expression restricts TGF-β production. HSC isolated from CB1 receptor knockout mice exhibit decreased phosphorylation of extracellular signal-regulated kinase (ERK) and Akt.[24]

Analyses using molecular and biological techniques have revealed that the phosphorylation status of several proteins, methylation of target genes, stability of mRNA and microRNA levels are involved in the activation of HSC and MFB. For instance, activation of HSC triggers the phosphorylation of Ser^{536} of the RelA subunit of NF-κB, which prevents the death of HSC. On the other hand, microRNA (miR) 132 hampers the transcription of CpG methylation protein, leading to the suppression of peroxisome proliferator-activated receptor (PPAR)-γ and MFB activation.[25] Mir-29b is reported to attenuate collagen 1A1 transcription in LX-2 cells, a human immortalized stellate cell line, independently of the Smad pathway, by binding to the 3′-untranslated region of its gene and also by downregulating a transcription factor, Sp-1.[26] Elevation of miR-29 was found to be increased in advanced fibrosis in human liver disease.[27]

Furthermore, genetic approaches have uncovered that the mutation of human genes, most frequently SNP, also relates to the progression of liver fibrosis; for instance, among SNP, Leu10Pro of TGF-β, Arg25Pro and G-6A of angiotensin, G-308A of tumor necrosis factor (TNF)-α, and C-592A/-819/G-1082A of IL-10 have been identified.[28] The 7-gene cirrhosis risk score (CRS), composed of seven different SNP, was reported to associate strongly with fibrosis progression.[29] Among the SNP in CRS, DDX5 S480A regulates the transcription of several genes in fibrosis in HSC.[30]

Regression of hepatic fibrosis

It is generally accepted that regression of liver fibrosis happens clinically in patients who achieve a sustained viral response (SVR) after the eradication of HCV by (pegylated) interferon (IFN) (+ ribavirin) therapy or whose HBV viral level is well controlled by using nucleot(s)ide analogs such as lamivudine, adefovir and entecavir. In addition, many clinical data indicate that not only cirrhosis can regress but also that this recovers the function of the liver and improves the prognosis of patients. Thus, the development of antifibrotic therapy is anticipated regardless of the etiology of liver disease.

Regression of liver fibrosis is mechanistically explained by the following four aspects: (i) regeneration of hepatocytes; (ii) retracing of activated and myofibroblast-like HSC to vitamin A-storing quiescent HSC; (iii) removal of MFB by apoptosis; and (iv) lysis of ECM. When hepatocyte necrosis takes place, the remaining hepatocytes undergo proliferation, leading to repair of the local environment. These processes are stimulated by growth factors derived from HSC, such as HGF, epidermal growth factor (EGF), epimorphin and pleiotrophin.[31] It is also indicated that neurotrophin signals are important as a paracrine loop between HSC and hepatocytes, and that Foxf1 forkhead transcription factor is involved in the process. On the other hand, retracing activated HSC to vitamin A-storing quiescent HSC is achieved at least in culture by forced overexpression of PPAR-γ or sterol regulatory element binding protein 1c (SREBP-1c) in activated HSC.[32] Regarding the removal of activated HSC or MFB, cul-

tured cells are sensitive to apoptosis induced by CD95 ligand and NK cell-derived TNF related apostosis including ligand (TRAIL). Apoptosis of activated HSC by hepatocyte-derived nerve growth factor (NGF) is regulated by a signal dependent on serotonin receptor. There is an interesting report describing the participation of NK cells in hepatic fibrogenesis; in a mouse model, depletion of NK cells using anti-asialo-GM1 antibody accelerates liver fibrosis and conversely, NK cell activation using poly I:C, a TLR3 ligand, attenuates the pathological process. Killing by NK cells is restricted to activated HSC which express NK cell-activating receptor NKG2D. Such involvement of NK cells in liver fibrosis is clinically observed in patients receiving liver transplantation; in patients taking immune-suppressing agents, such as cyclosporine and glucocorticoid, liver fibrosis progresses at an increasing rate after liver transplantation.[33]

Matrix-metalloproteinases are calcium-dependent enzymes that digest ECM. MMP are classified into: (i) interstitial collagenases (MMP-1, -8, -13); (ii) gelatinase (MMP-2 and -9); (iii) stromelysin (MMP-3, -7, -10, -11); (iv) membrane type (MMP-14, -15, -16, -17, -24, -25); and (v) metalloelastase (MMP-12). HSC secrete MMP-2, -9 and -13 (in humans, MMP-1), and stromelysin. Because MMP-1 is a key collagenase that metabolizes type I collagen, it is the principal element to the improved fibrotic status of the liver; however, MMP activity also strictly regulates its binding partner, TIMP. Because HSC are able to generate both TIMP-1 and -2, a local balance between MMP and TIMP offer a key to solve the fibrotic process.[34] It is interesting to note that human T-cell-derived microparticles in the blood of hepatitis patients induce fibrolytic activity of HSC.[35]

Therapy for liver fibrosis

Information obtained by molecular analyses of liver fibrogenesis, in particular the activation process of HSC and MFB, facilitates the establishment of regulatory methods of human liver fibrosis and, currently, a clinical trial using a new compound, GI262570, is underway (see http://clinicaltrials.gov/). In chronic hepatitis C, IFN-based therapy has progressed markedly and the SVR rate after therapy has approached 50–60% even in difficult-to-treat patients with genotype 1, high viral load. SVR is expected to reach 70–90% in the near future by using additional protease or polymerase inhibitors. Regarding chronic hepatitis B, liver fibrosis progression is ameliorated in patients treated by nucleot(s)ide analogs, while mutation of HBV by elongation of the therapy period is far from reassuring. However, antifibrotic therapies that are safe, have minimal side-effects and can be given for a long time are definitely required in patients who have failed to achieve SVR with previous IFN therapy for chronic hepatitis C and who have an advanced fibrotic stage, such as cirrhosis, in any kind of liver disease, including NASH, a risk factor for non-B/non-C cirrhosis. These patients should be treated for a better prognosis of cirrhosis and to prevent the occurrence of HCC.

Strategies for antifibrotic therapy include: (i) regulation of the activation of HSC and MFB; (ii) suppression of collagen production by them; (iii) control of their proliferation; and (iv) regulation of stroma and neovascularization. IFN-α and -β, which are clinically used to eradicate HCV and HBV, are known to regulate promoters of collagen gene expression by way of intracellular signaling molecules, such as signal transducers and activators of transcription-1 (Stat-1) and p300.[36] As stated above, IFN is able to regulate collagen gene expression in HSC through inducing microRNA-29b.[26] Pegylated-IFN-α is retained in the circulation for a longer period than the conventional IFN and may activate the type I IFN receptor (IFNAR)-dependent Janus kinase/Stat-1 pathway, resulting in the augmented suppression of HSC.

Newly developed anticancer agents target tumor stroma that support tumor growth and survival through neovascularization.[37] Sorafenib and other multi-kinase inhibitors in clinical trials inhibit receptor-tyrosine kinase and Raf–MEK (MAPK Extracellular Signal-Related Kinase)–ERK signaling pathways that are activated by the binding of VEGF, fibroblast growth factor, PDGF and other growth factors to their individual receptors.[38] The septum of fibrotic liver is composed of capillaries with vascular endothelial cells and "pericytic" activated HSC and MFB. Thus, molecular-targeted anticancer agents themselves are anticipated to have antifibrotic potential.[39]

Evaluation of liver fibrosis

While liver fibrosis research has raised enthusiasm in the area of mechanistic analyses and therapeutic approaches, clinical diagnosis has also made marked progression. Because liver tissues obtained at liver biopsy are equivalent to 1/50 000, this small part of the liver does not always reflect the condition of the whole liver. Thus, it is necessary to solve several problems related to liver biopsy and to develop a method of evaluating the stage of liver fibrosis non-invasively.[40]

NEW TOOLS TO EVALUATE LIVER FIBROSIS

Serum tests

IN CLINICAL PRACTICE, type IV collagen 7 S, type III procollagen N-terminal peptide (P-III-P) and hyarulonic acid are commonly utilized as serum markers for human liver fibrosis, although it is difficult to distinguish each pathological fibrosis stage using one of these ECM products. On the other hand, the European Liver Fibrosis (ELF) study reported a marker composed of the combination of P-III-P, hyarulonic acid, and TIMP-1, which achieved the diagnostic power of area under the curve (AUC) 0.80 for Scheuer 3–4.[41] Independently of these "direct" serum markers originating from ECM degradation, "indirect" serum estimation markers of liver fibrosis have been reported including AAR (aspartate aminotransferase [AST]/alanine aminotransferase [ALT] ratio), APRI (AST-to-platelet ratio index), CDS (cirrhosis discriminant score), fibrotest and the HALT-C model, which are composed of plural parameters commonly measured in clinical practice. Fibrotest is an algorithm composed of six parameters – haptoglobin, α2-macroglobulin, apolipoprotein-A1, γ-glutamyltransferase, bilirubin, and γ-globulin – and its diagnostic power for more than F2-4 was reported to be AUC 0.87. Fibrometer is a numerical formula composed of the platelet count, prothrombin time, AST, hyarulonic acid, α2-macroglobulin, sex and age, and its diagnostic power for more than F2-4 was reported to be AUC 0.89.[42] The advantage of these serum tests is to determine mild fibrosis or cirrhosis at a rate of more than 50% without liver biopsy, while they have less accuracy in the stepwise discrimination of each stage of moderate fibrosis (F1–F2, F2–F3, and F3–F4) (Table 1).[43]

Evaluation of liver fibrosis using ultrasound-based technology

Transient elastography

Transient elastography, FibroScan502, was developed by ECOSENS (Paris, France) to evaluate liver fibrosis non-invasively in a short examination, measuring using ultrasonography, the propagation of low energy 3.5-MHz signals of a mechanical shear wave through liver tissue. This machine evaluates the stiffness of 3 cm^3 liver, implying that it covers at least a 100-times larger volume of liver tissue than liver biopsy. In particular, this device has been used to evaluate liver stiffness in chronic hepatitis C with good correlation to the F stage of the Metavir score and Inuyama classification. A report from Castera *et al.* in 2005 was pioneering;[44] the diagnostic accuracy of liver stiffness measurement as evaluated by Area Under Receiver Operating Characteristic Curve (AUROC) ranges was 0.84 for the diagnosis of significant fibrosis (≥F2), 0.90 for the diagnosis of advanced fibrosis (≥F3) and 0.94 for the diagnosis of cirrhosis. Recent publications have indicated that liver stiffness measurement is also applied for the evaluation of liver fibrosis in hepatitis B and NASH, while careful attention is required in cases of acute inflammation (acute hepatitis) or flares because the value of liver stiffness increases independently of the stage of liver fibrosis in these cases.[45,46]

Real-time tissue elastography

Real-time tissue elastography is a new diagnostic tool for the evaluation of tissue elasticity based on ultrasound technology, and was developed by Hitachi Medical (Tokyo, Japan). Real-time tissue elastography can be performed when patients undergo common B-mode screening of the liver by ultrasonography. It is already utilized to detect space-occupying lesions in mammary glands, the thyroid and prostate because tumors have abnormal elasticity compared to surrounding intact tissue. The computer-assisted apparatus calculates the relative hardness of tissue from the degree of tissue distortion and displays this information as a color image. Although ultrasound elastography does not reflect physical elasticity directly, it indicates the relative degree of tissue strain under subtle compression (Fig. 3). Frriedrich-Rust *et al.* applied this technique to measure liver stiffness and reported its usefulness for the diagnosis of significant fibrosis (for >F2, AUC 0.93) in combination with APRI.[47] The AUROC power of real-time tissue elastography was reported to be similar to that of transient elastography in patients with chronic hepatitis C.[48] Because real-time tissue elastography can be performed simultaneously with B-mode ultrasonography and applied for patients with obesity and ascites, it could be used widely in clinical practice more than transient elastography.

Acoustic radiation force impulse (ARFI)

Most recent technology is ARFI. This examination is performed at the time of B-mode observation of ultrasonography, similarly to real-time tissue elastography. This method is based on the generation and spreading of the shear wave within tissues after giving a "pushing pulse" of focused, impulsive and acoustic radiation force impulse. The harder the tissue is, the faster the shear wave spreads. Previous reports have indicated that

Table 1 Serum fibrosis markers

Index	Parameters	CLD and number of patients	Calculation	Interpretation	PPV/NPV (%)	AUC
Foms	Age, plt, γGT, cholesterol	HCV: t = 351 v = 125	7.811 – 3.131 × ln (plt) + 0.781 × ln (γGT) + 3.467 × ln (age) – 0.014 (cholesterol)	>6.9 = Scheuer 2–4 <4.2 = Scheuer 0–1	PPV = 66 NPV = 96	t = 0.86 v = 0.81
APRI	AST, plt	HCV: t = 192 v = 78	([AST / ULN] / plt [×10⁹/L]) × 100	>1.5 = Ishak 3–6 ≤0.5 = Ishak 0–2	PPV = 91 NPV = 90	t = 0.80 v = 0.88
FT, FS	Haptoglobin, α2-MC, apo-A1	HCV, HBV: t = 205 v = 134	Logistic regression index (proprietary)	0.75–1.00 = F4 0.73–0.74 = F3–F4 0.59–0.72 = F3 0.49–0.58 = F2 0.32–0.48 = F1–F2 0.28–0.31 = F1 0.22–0.27 = F0–F1 0.00–0.21 = F0	PPV = 78 PPV = 76 PPV = 76 PPV = 67 PPV/NPV = 61/85 NPV = 91 NPV = 92 NPV = 94	≥F2–F4 t = 0.83 v = 0.87
Fibroindex	Plt, AST, γGT	HCV: t = 240 v = 120	1.738 – 0.064 (plt [×10⁴/mm³]) + 0.005 (AST [IU/L]) + 0.463 × (γGT [g/dL])	≤1.25 = F0–F1 ≥2.25 = F2–F3	NPV = 61.7 PPV = 90	t = 0.83 v = 0.82
FIB-4	Plt, AST, ALT, age	HCV or HIV: t = 555 v = 277	(Age × AST) / (plt count × ALT$^{1/2}$)	<1.45 = Ishak <4–6 >3.25 = Ishak ≥4–6	NPV = 90 PPV = 65	0.76
Virahep-C model	AST, plt, ALP, age	HCV: 399	1 / (exp [–y] + 1) with y = –5.17 + 0.20 × race + 0.07 × age (years) + 1.19 × ln (AST – 1.76) × ln (plt [×10³/mL]) + 1.38 × ln (ALP)	>0.55 = Ishak 3–6 ≤0.22 = Ishak 0–2	NPV = 85 PPV = 81	0.83
GUCI	AST, INR, plt	HCV: 179	AST × prothrombin-INR × 100 / plt (×10³/L)	>1.0 = Ishak ≥4–6	NPV = 31 PPV = 97	0.85
Hui	BMI, bilirubin, plt, albumin	HBV: t = 150 v = 85	exp (3.148 + 0.167 × BMI + 0.088 × bilirubin [μM] – 0.151 × albumin [g/L] – 0.019 × plt [×10⁹/L]) / (1 + exp (3.148 + 0.167 × BMI + 0.088 × bilirubin [μM] – 0.151 × albumin [g/L] – 0.019 × plt [×10⁹/L])	>0.5 = Ishak 3–6 ≤0.15 = Ishak 0–2	NPV = 81 PPV = 53 NPV = 92 PPV = 38	t = 0.80 v = 0.77
Mohamadenjad	Albumin, plt, ALP, HBV DNA	HBV: t = 130 v = 99	10 + (0.771 × $\log_{10}$ HBV DNA copies/mL) + (3.828 × $\log_{10}$ (ALP / ULN) (1.066 albumin g/dL) – (0.011 [plt/1000 μL])	<4.72 = Ishak <4–6 >7.75 = Ishak ≥4–6	NPV = 99 PPV = 26 NPV = 93 PPV = 75	t = 0.91 v = 0.85

α2-MC, α2-macroglobulin; ALP, alkaline phosphatase; AST, aspartate aminotransferase; AUC, area under the curve; BMI, body mass index; CLD, chronic liver disease; γGT, γ-glutamyl transpeptidase; HBV, hepatitis B virus; HCV, hepatitis C virus; INR, international normalized ratio; NPV, negative predictive value; plt, platelets; PPV, positive predictive value; ULN, upper limit of normal.

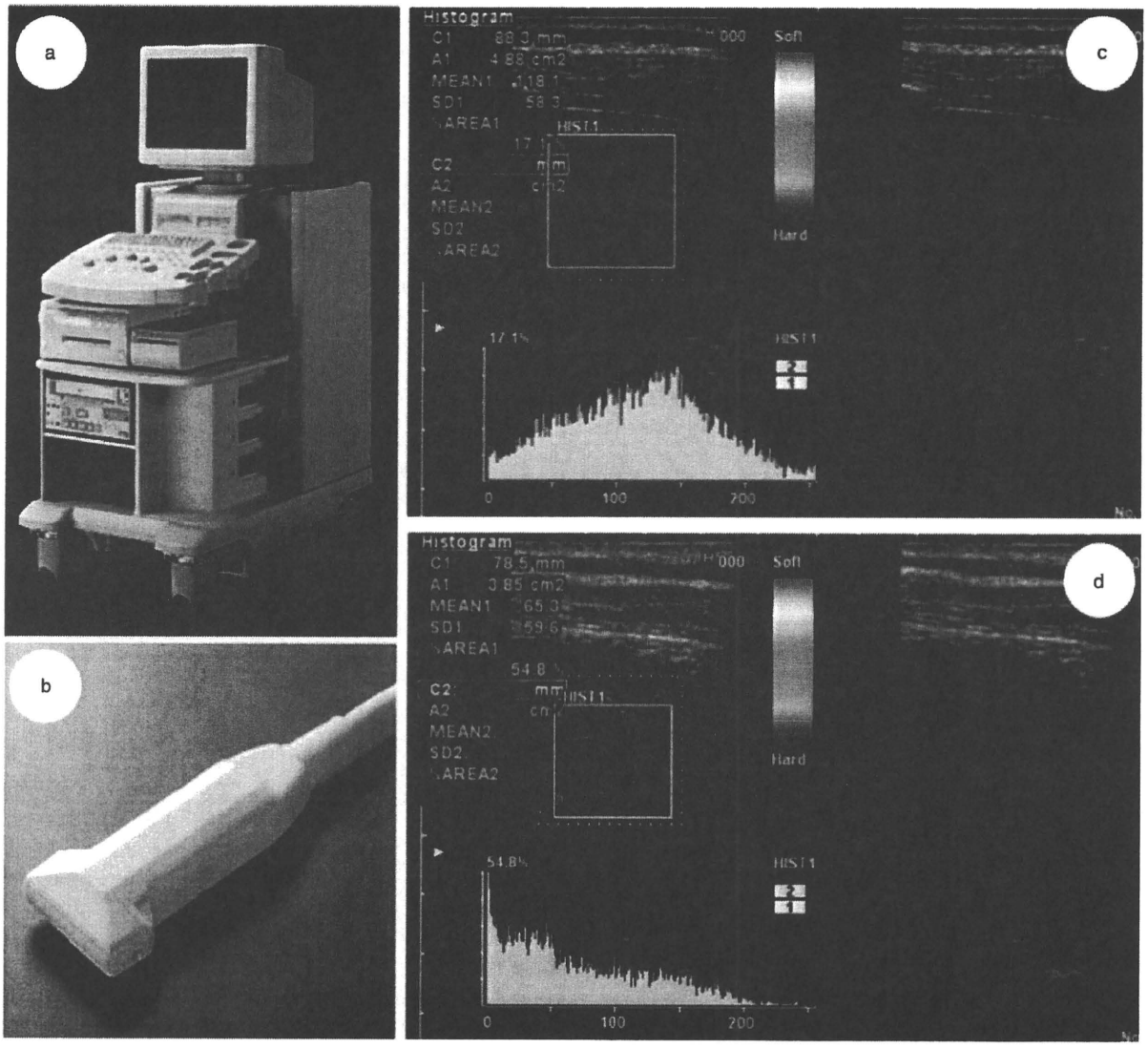

Figure 3 Real-time tissue elastography. (a) Ultrasonography machine. (b) Probe for real-time tissue elastography. (c) RTE color image of F1 patient with liver stiffness of 6.9 kPa obtained by transient elastography (FibroScan). (d) RTE color image of F4 patient with liver stiffness of 33.3 kPa obtained by transient elastography (FibroScan). RTE, real-time tissue elastography.

the diagnostic power of ARFI for the staging of liver fibrosis is the same as that of transient elastography.[49]

APPLICATION OF LIVER STIFFNESS MEASUREMENT FOR THE SCREENING OF HCC AND CIRRHOSIS COMPLICATIONS

EVALUATION OF LIVER fibrosis in chronic liver disorders is useful in determining disease progression and assessing complications, such as HCC and esophageal varices. Foucher *et al.* reported that, in 144 chronic hepatitis C patients with fibrosis stages F3 or F4, the cut-off values of liver stiffness (kPa) measured by transient elastography were 27.5, 49.1, 53.7 and 62.7 for the appearance of esophageal varices (stage 2/3), ascites, HCC and rupture of esophageal varices.[50]

Masuzaki *et al.* prospectively observed that, in 866 patients with chronic hepatitis C, HCC developed within 3 years of observation in 77 cases, and liver stiffness at entry was less than 10 kPa in 0.4% and more

than 25 kPa in 38.5%, indicating the usefulness of liver stiffness measurement as a tool for forecasting the development of HCC.[51]

CONCLUSION

LIVER FIBROSIS RESEARCH was initiated to explore the unknown functions of HSC and MFB, has advanced simultaneously in both basic and clinical aspects, and has achieved the non-invasive assessment of the diagnosis of liver fibrosis, identifying a new compound that is therapeutically appropriate. Future progression and expansion of this research field is eagerly anticipated.

ACKNOWLEDGMENT

THIS WORK WAS supported by a grant from the Ministry of Health, Labor and Welfare of Japan to N. Kawada (2008–2010).

REFERENCES

1 Friedman SL, Roll FJ, Boyles J, Bissell DM. Hepatic lipocytes: the principal collagen-producing cells of normal rat liver. *Proc Natl Acad Sci USA* 1985; **82**: 8681–5.
2 Friedman SL. Evolving challenges in hepatic fibrosis. *Nat Rev Gastroenterol Hepatol* 2010; **7**: 425–36.
3 Villanueva A, Minguez B, Forner A, Reig M, Llovet JM. Hepatocellular carcinoma: novel molecular approaches for diagnosis, prognosis, and therapy. *Annu Rev Med* 2010; **61**: 317–28.
4 Starley BQ, Calcagno CJ, Harrison SA. Nonalcoholic fatty liver disease and hepatocellular carcinoma: a weighty connection. *Hepatology* 2010; **51**: 1820–32.
5 Gane EJ, Roberts SK, Stedman CA *et al.* Oral combination therapy with a nucleoside polymerase inhibitor (RG7128) and danoprevir for chronic hepatitis C genotype 1 infection (INFORM-1): a randomised, double-blind, placebo-controlled, dose-escalation trial. *Lancet* 2010; **376**: 1467–75.
6 Wake K. Perisinusoidal stellate cells (fat-storing cells, interstitial cells, lipocytes), their related structure in and around the liver sinusoids, and vitamin A-storing cells in extrahepatic organs. *Int Rev Cytol* 1980; **66**: 303–53.
7 Kawada N, Tran-Thi TA, Klein H, Decker K. The contraction of hepatic stellate (Ito) cells stimulated with vasoactive substances. Possible involvement of endothelin 1 and nitric oxide in the regulation of the sinusoidal tonus. *Eur J Biochem* 1993; **213**: 815–23.
8 Friedman SL. Hepatic stellate cells: protean, multifunctional, and enigmatic cells of the liver. *Physiol Rev* 2008; **88**: 125–72.
9 Mann DA, Marra F. Fibrogenic signalling in hepatic stellate cells. *J Hepatol* 2010; **52**: 949–50.
10 Choi SS, Syn WK, Karaca GF *et al.* Leptin promotes the myofibroblastic phenotype in hepatic stellate cells by activating the hedgehog pathway. *J Biol Chem* 2010; **285**: 36551–60.
11 Forbes SJ, Russo FP, Rey V *et al.* A significant proportion of myofibroblasts are of bone marrow origin in human liver fibrosis. *Gastroenterology* 2004; **126**: 955–63.
12 Kisseleva T, Uchinami H, Feirt N *et al.* Bone marrow-derived fibrocytes participate in pathogenesis of liver fibrosis. *J Hepatol* 2006; **45**: 429–38.
13 Dranoff JA, Wells RG. Portal fibroblasts: underappreciated mediators of biliary fibrosis. *Hepatology* 2010; **51**: 1438–44.
14 Zeisberg M, Yang C, Martino M *et al.* Fibroblasts derive from hepatocytes in liver fibrosis via epithelial to mesenchymal transition. *J Biol Chem* 2007; **282**: 23337–47.
15 Scholten D, Osterreicher CH, Scholten A *et al.* Genetic labeling does not detect epithelial-to-mesenchymal transition of cholangiocytes in liver fibrosis in mice. *Gastroenterology* 2010; **139**: 987–98.
16 Taura K, Miura K, Iwaisako K *et al.* Hepatocytes do not undergo epithelial-mesenchymal transition in liver fibrosis in mice. *Hepatology* 2010; **51**: 1027–36.
17 Jiang JX, Venugopal S, Serizawa N *et al.* Reduced nicotinamide adenine dinucleotide phosphate oxidase 2 plays a key role in stellate cell activation and liver fibrogenesis in vivo. *Gastroenterology* 2010; **139**: 1375–84.
18 Kim SY, Cho BH, Kim UH. CD38-mediated Ca2+ signaling contributes to angiotensin II-induced activation of hepatic stellate cells: attenuation of hepatic fibrosis by CD38 ablation. *J Biol Chem* 2010; **285**: 576–82.
19 Seki E, De Minicis S, Osterreicher CH *et al.* TLR4 enhances TGF-beta signaling and hepatic fibrosis. *Nat Med* 2007; **13**: 1324–32.
20 Syn WK, Choi SS, Liaskou E *et al.* Osteopontin is induced by hedgehog pathway activation and promotes fibrosis progression in nonalcoholic steatohepatitis. *Hepatology* 2011; **53**: 106–15.
21 Sahin H, Trautwein C, Wasmuth HE. Functional role of chemokines in liver disease models. *Nat Rev Gastroenterol Hepatol* 2010; **7**: 682–90.
22 Syn WK, Oo YH, Pereira TA *et al.* Accumulation of natural killer T cells in progressive nonalcoholic fatty liver disease. *Hepatology* 2010; **51**: 1998–2007.
23 Hézode C, Zafrani ES, Roudot-Thoraval F *et al.* Daily cannabis use: a novel risk factor of steatosis severity in patients with chronic hepatitis C. *Gastroenterology* 2008; **134**: 432–9.
24 Mallat A, Lotersztajn S. Cannabinoid receptors as novel therapeutic targets for the management of non-alcoholic steatohepatitis. *Diabetes Metab* 2008; **34**: 680–4.
25 Mann J, Chu DC, Maxwell A *et al.* MeCP2 controls an epigenetic pathway that promotes myofibroblast

transdifferentiation and fibrosis. *Gastroenterology* 2010; **138**: 705–14.
26 Ogawa T, Iizuka M, Sekiya Y *et al.* Suppression of type I collagen production by microRNA-29b in cultured human stellate cells. *Biochem Biophys Res Commun* 2010; **391**: 316–21.
27 Roderburg C, Urban GW, Bettermann K *et al.* Micro-RNA profiling reveals a role for miR-29 in human and murine liver fibrosis. *Hepatology* 2011; **53**: 209–18.
28 Hold GL, Untiveros P, Saunders KA *et al.* Role of host genetics in fibrosis. *Fibrogenesis Tissue Repair* 2009; **2**: 6.
29 Huang H, Shiffman ML, Friedman S *et al.* A 7 gene signature identifies the risk of developing cirrhosis in patients with chronic hepatitis C. *Hepatology* 2007; **46**: 297–306.
30 Guo J, Hong F, Loke J *et al.* A DDX5 S480A polymorphism is associated with increased transcription of fibrogenic genes in hepatic stellate cells. *J Biol Chem* 2010; **285**: 5428–37.
31 Sawitza I, Kordes C, Reister S, Häussinger D. The niche of stellate cells within rat liver. *Hepatology* 2009; **50**: 1617–24.
32 She H, Xiong S, Hazra S *et al.* Adipogenic transcriptional regulation of hepatic stellate cells. *J Biol Chem* 2005; **280**: 4959–67.
33 Gawrieh S, Papouchado BG, Burgart LJ *et al.* Early hepatic stellate cell activation predicts severe hepatitis C recurrence after liver transplantation. *Liver Transpl* 2005; **11**: 1207–13.
34 Benyon RC, Arthur MJ. Extracellular matrix degradation and the role of hepatic stellate cells. *Semin Liver Dis* 2001; **21**: 373–84.
35 Kornek M, Popov Y, Libermann TA, Afdhal NH, Schuppan D. Human T cell microparticles circulate in blood of hepatitis patients and induce fibrolytic activation of hepatic stellate cells. *Hepatology* 2011; **53**: 230–42.
36 Inagaki Y, Nemoto T, Kushida M *et al.* Interferon alfa down-regulates collagen gene transcription and suppresses experimental hepatic fibrosis in mice. *Hepatology* 2003; **38**: 890–9.
37 Whittaker S, Marais R, Zhu AX. The role of signaling pathways in the development and treatment of hepatocellular carcinoma. *Oncogene* 2010; **29**: 4989–500.
38 Wang Y, Gao J, Zhang D, Zhang J, Ma J, Jiang H. New insights into the antifibrotic effects of sorafenib on hepatic stellate cells and liver fibrosis. *J Hepatol* 2010; **53**: 132–44.
39 Mejias M, Garcia-Pras E, Tiani C, Miquel R, Bosch J, Fernandez M. Beneficial effects of sorafenib on splanchnic, intrahepatic, and portocollateral circulations in portal hypertensive and cirrhotic rats. *Hepatology* 2009; **49**: 1245–56.
40 Pinzani M, Vizzutti F, Arena U, Marra F. Technology Insight: noninvasive assessment of liver fibrosis by biochemical scores and elastography. *Nat Clin Pract Gastroenterol Hepatol* 2008; **5**: 95–106.
41 Guha IN, Parkes J, Roderick P *et al.* Noninvasive markers of fibrosis in nonalcoholic fatty liver disease: validating the European Liver Fibrosis Panel and exploring simple markers. *Hepatology* 2008; **47**: 455–60.
42 Ngo Y, Munteanu M, Messous D *et al.* A prospective analysis of the prognostic value of biomarkers (FibroTest) in patients with chronic hepatitis C. *Clin Chem* 2006; **52**: 1887–96.
43 Parkes J, Roderick P, Harris S *et al.* Enhanced Liver Fibrosis (ELF) Test can predict clinical outcomes in patients with mixed aetiology chronic liver disease. *Gut* 2010; **59**: 1245–51.
44 Castéra L, Vergniol J, Foucher J *et al.* Prospective comparison of transient elastography, Fibrotest, APRI, and liver biopsy for the assessment of fibrosis in chronic hepatitis C. *Gastroenterology* 2005; **128**: 343–50.
45 Wong VW, Vergniol J, Wong GL *et al.* Diagnosis of fibrosis and cirrhosis using liver stiffness measurement in nonalcoholic fatty liver disease. *Hepatology* 2010; **51**: 454–62.
46 Dechêne A, Sowa JP, Gieseler RK *et al.* Acute liver failure is associated with elevated liver stiffness and hepatic stellate cell activation. *Hepatology* 2010; **52**: 1008–16.
47 Friedrich-Rust M, Ong MF, Herrmann E *et al.* Real-time elastography for noninvasive assessment of liver fibrosis in chronic viral hepatitis. *AJR Am J Roentgenol* 2007; **188**: 758–64.
48 Morikawa H, Fukuda K, Kobayashi S *et al.* Real-time tissue elastography as a tool for the noninvasive assessment of liver stiffness in patients with chronic hepatitis C. *J Gastroenterol* 2010; Aug 10. [Epub ahead of print]
49 Yoneda M, Suzuki K, Kato S *et al.* Nonalcoholic fatty liver disease: US-based acoustic radiation force impulse elastography. *Radiology* 2010; **256**: 640–7.
50 Castéra L, Foucher J, Bernard PH *et al.* Pitfalls of liver stiffness measurement: a 5-year prospective study of 13,369 examinations. *Hepatology* 2010; **51**: 828–35.
51 Masuzaki R, Tateishi R, Yoshida H *et al.* Prospective risk assessment for hepatocellular carcinoma development in patients with chronic hepatitis C by transient elastography. *Hepatology* 2009; **49**: 1954–61.

Original Article

Down-regulation of cyclin E1 expression by microRNA-195 accounts for interferon-β-induced inhibition of hepatic stellate cell proliferation

Yumiko Sekiya[1, 2], Tomohiro Ogawa[1, 2], Masashi Iizuka[1, 2], Katsutoshi Yoshizato[1, 2, 3], Kazuo Ikeda[4], and Norifumi Kawada[1, 2, *]

Departments of [1]Hepatology and [2]Liver Research Center, Graduate School of Medicine, Osaka City University, Osaka, Japan

[3]PhoenixBio Co. Ltd., Hiroshima, Japan

[4]Department of Anatomy and Cell Biology, Graduate School of Medical Sciences, Nagoya City University, Aichi, Japan

* Correspondence to: Norifumi Kawada, MD & PhD, Department of Hepatology, Graduate School of Medicine, Osaka City University, 1-4-3, Asahimachi, Abeno, Osaka 545-8585, Japan. Phone: +81 6 6645 3897; Fax: +81 6 6646 6072; E-mail: kawadanori@med.osaka-cu.ac.jp

Received 6 September 2010; Revised 18 November 2010; Accepted 3 December 2010
Journal of Cellular Physiology

DOI 10.1002/jcp.22598

Running head: antiproliferative effect of IFN-β via miR-195

Keywords: cell cycle, p21, liver fibrosis, LX-2, miR-16 family

Contract grant sponsor: The Ministry of Health, Labour and Welfare of Japan

Contract grant number: 2008-KAKEN-IPPAN-003

Abstract

Recent studies have suggested that interferons (IFNs) have an antifibrotic effect in the liver independent of their antiviral effect although its detailed mechanism remains largely unknown. Some microRNAs have been reported to regulate pathophysiological activities of hepatic stellate cells (HSCs). We performed analyses of the antiproliferative effects of IFNs in HSCs with special regard to microRNA-195 (miR-195). We found that miR-195 was prominently down-regulated in the proliferative phase of primary-cultured mouse HSCs. Supporting this fact, IFN-β induced miR-195 expression and inhibited the cell proliferation by delaying their G1 to S phase cell cycle progression in human HSC line LX-2. IFN-β down-regulated cyclin E1 and up-regulated p21 mRNA levels in LX-2 cells. Luciferase reporter assay revealed the direct interaction of miR-195 with the cyclin E1 3'UTR. Overexpression of miR-195 lowered cyclin E1 mRNA and protein expression levels, increased p21 mRNA and protein expression levels, and inhibited cell proliferation in LX-2 cells. Moreover miR-195 inhibition restored cyclin E1 levels that were down-regulated by IFN-β. In conclusion, IFN-β inhibited the proliferation of LX-2 cells by delaying cell cycle progression in G1 to S phase, partially through the down-regulation of cyclin E1 and up-regulation of p21. IFN-induced miR-195 was involved in these processes. These observations reveal a new mechanistic aspect of the antifibrotic effect of IFNs in the liver.

Introduction

Hepatic fibrosis is characterized by excessive accumulation of extracellular matrices (ECM) and is a common feature of chronic liver diseases. Hepatic stellate cells (HSCs) are considered to play multiple roles in the fibrotic process. HSCs maintain a quiescent phenotype and store vitamin A under physiological conditions. When liver injury occurs, they become activated and trans-differentiate into myofibroblastic cells, whose characteristics include the proliferation, loss of vitamin A droplets, expression of α-smooth muscle actin (α-SMA), secretion of profibrogenic mediators and ECM (Bataller and Brenner, 2001; Friedman, 2000). Therefore, controlling the population and activation of HSCs should be a potential therapeutic target against liver fibrosis.

Interferons (IFNs) are cytokines with antiviral, immunomodulatory, and cell growth inhibitory effects. IFN-α and -β are classified as type I IFNs (Pestka et al., 1987; Uze et al., 2007), which are generally applied for the therapy of eradication of hepatitis B and C viruses. Studies using rodent models and cultured HSCs have also suggested that IFNs have a direct antifibrotic potential independently of their antivirus activity (Chang et al., 2005; Fort et al., 1998; Inagaki et al., 2003; Mallat et al., 1995; Ogawa et al., 2009; Shen et al., 2002; Tanabe et al., 2007), although the detailed molecular mechanisms of these effects of IFNs remain to be clarified.

Recently, microRNAs (miRNAs), which are endogenous small non-coding RNA, have become a focus of interest as post-transcriptional regulators of gene expression through interaction with the 3' untranslated region (3'UTR) of target mRNAs (Bartel, 2004). miRNAs are known to participate in cell proliferation, development, differentiation, and metabolism (Bartel, 2004). Moreover, it has been reported that expression of miRNAs

could alter hepatic pathophysiology; miR-122 is involved in the IFN-β-related defense system against viral hepatitis C (Pedersen et al., 2007), and miR-26 is associated with survival and response to adjuvant IFN-α therapy in patients with hepatocellular carcinoma (HCC) (Ji et al., 2009a). Regarding HSCs, miR-15b and miR-16 are down-regulated upon HSC's activation, and their overexpression induces apoptosis and a delay in the cell cycle (Guo et al., 2009a; Guo et al., 2009b). Knockdown of miR-27a and miR-27b in activated HSCs allowed a switch to a more quiescent phenotype and decreased cell proliferation (Ji et al., 2009b). miR-150 and miR-194 suppress proliferation, activation, and ECM production of HSCs (Venugopal et al., 2010). Recently, we showed that miR-29b was induced by IFN and suppressed type I collagen production in LX-2 cells (Ogawa et al., 2010).

In the present study, we measured the levels of miR-195 in primary-cultured mouse HSCs and found that its expression was markedly reduced in their activation phase, suggesting the regulatory role of miR-195 in the activation/deactivation process of HSCs. Because miR-195 is categorized into the same family as miR-15b and miR-16 and has been reported to regulate cell cycle by targeting E2F3, CDK6, and cyclin D1 (Xu et al., 2009), we suspect the involvement of miR-195 in the proliferation of HSC and in type I IFN, in particular IFN-β, -induced inhibition of their growth.

Materials and Methods

Materials. Human hepatic stellate cell line LX-2 was donated by Dr. Scott L. Friedman (Mount Sinai School of Medicine, New York, NY, USA) (Xu et al., 2005). Necessary reagents and materials were obtained from the following sources: Dulbecco's

modified Eagle's medium (DMEM) from Sigma Chemical Co. (St. Louis, MO, USA); fetal bovine serum (FBS) from Invitrogen (Carlsbad, CA, USA); human natural IFN-α and IFN-β from Otsuka Pharmaceutical Co. (Tokushima, Japan) and Toray Industries Inc. (Tokyo, Japan), respectively; precursor and inhibitor of miR-195, and the corresponding negative controls from Ambion (Austin, TX, USA); mouse monoclonal antibody against cyclin E1, cyclin D1 and p21, and glyceraldehyde-3-phosphate dehydrogenase (GAPDH) from MBL (Nagoya, Japan), Cell Signaling Technology Inc. (Beverly, MA, USA), and Chemicon International Inc. (Temecula, CA, USA), respectively; rabbit polyclonal antibodies against cyclin-dependent kinase (CDK) 6 and E2F3 from Santa Cruz Biotechnology Inc. (Santa Cruz, CA, USA); goat polyclonal antibody against CDK4 from Santa Cruz Biotechnology Inc.; enhanced Chemiluminescence plus detection reagent from GE Healthcare (Buckinghamshire, UK); Immobilon P membranes from Millipore Corp. (Bedford, MA, USA); reagents for cDNA synthesis and real-time PCR from Toyobo (Osaka, Japan); a cell counting kit from Dojindo Laboratories (Kumamoto, Japan); and all other reagents from Sigma Chemical Co. or Wako Pure Chemical Co. (Osaka, Japan).

Cells. LX-2 cells were maintained in DMEM supplemented with 10% FBS (DMEM/FBS) and were plated at a density of 0.7–1.5 × 10^4 cells/cm^2 24 h prior to biological assay. Biological assays were done in DMEM/FBS unless stated otherwise. Mouse primary HSCs were isolated from male C57BL/6 mice by the pronase-collagenase digestion method as described previously (Uyama et al., 2006) and were cultured in DMEM/FBS.

Transient transfection of miRNA precursors and inhibitors. Precursor of miR-195,

which was a double-strand RNA mimicking endogenous miR-195 precursor, and the negative control with a scrambled sequence were transfected into LX-2 cells using Lipofectamine 2000 (Invitrogen) at a final concentration of 50 nM in accordance with the manufacturer's instructions. Briefly, miRNA precursor and Lipofectamine 2000 were mixed at a ratio of 25 (pmol):1 (μl) in Opti-MEM I Reduced Medium (Invitrogen), incubated for 20 min at room temperature, and were then added to the cultures. After 24 h, the culture medium was replaced with fresh medium. Inhibitor of miR-195, which was designed to bind to endogenous miR-195 and inhibit its activity, and the negative control with a scrambled sequence were transfected similarly. After 6 h, the culture medium was changed and IFN-β was added successively.

Cell proliferation assay. LX-2 cells were plated at a density of 2×10^3 cells/well in 96-well plates 24 h prior to experiments. The culture medium was replaced by fresh medium containing different concentrations of IFNs at day 0 and 3. After 3, 5, and 7 days of treatment, cell proliferation was measured by WST-1 assay. In another experiment, the cells were plated at a density of 3×10^3 cells/well in 96-well plate for 24 h prior and were then transfected with the miR-195 precursor as described above. After 24 h, the medium was changed and the culture was continued for an additional 1–3 days before the measurement of cell proliferation.

Cell cycle analysis. Cells were serum starved for 24 h and then the medium was replaced with IFN-containing DMEM/FBS. At the indicated time points after treatment, the cells were harvested by trypsinization, washed in phosphate buffered saline (PBS), and fixed in ice-cold 70% ethanol. The cells were washed in PBS and resuspended in PBS containing 500 μg/ml RNase A and incubated for 20 min. Cellular DNA was

stained with propidium iodide at a final concentration of 25 μg/ml for 20 min. The cells were analyzed using a FACSCalibur HG flow cytometer (Becton Dickinson, Franklin Lakes, NJ, USA). A total of 20,000 events were counted for each sample. Data were analyzed using ModFIT LT software (Verity Software House, Topsham, ME, USA).

Quantitative real-time PCR. Quantitative real-time PCR was performed according to the method described elsewhere with use of a set of gene-specific oligonucleotide primers (Table 1) using an Applied Biosystems Prism 7500 (Applied Biosystems, Foster City, CA, USA) (Ogawa et al., 2010). To detect miR-195 expression, the reverse transcription reaction was performed using a TaqMan microRNA Assay (Applied Biosystems) in accordance with the manufacturer's instructions. The expression level of GAPDH was used to normalize the relative abundance of mRNAs and miR-195.

Immunoblotting. Cells were lysed in RIPA buffer [50 mM Tris/HCl, pH7.5, 150 mM NaCl, 1% NP-40, 0.5% sodium deoxycholate, 0.1% sodium dodecyl sulfate (SDS)] containing Protease Inhibitor Cocktail, Phosphatase Inhibitors Cocktail 1, and Phosphatase Inhibitor Cocktail 2 (Sigma). Proteins (20 μg) were electrophoresed in a 10% SDS-polyacrylamide gel and then transferred onto Immobilon P membranes (Ogawa et al., 2010). Immunoreactive bands were visualized by the enhanced chemiluminescence system using a Fujifilm Image Reader LAS-3000 (Fuji Medical Systems, Stamford, CT, USA).

Luciferase reporter assay. Interaction of miR-195 to the 3'UTR of the cyclin E1 gene was tested according to the reported method (Ogawa et al., 2010). The 3'UTR of the cyclin E1 gene containing putative miR-195 target regions was obtained by PCR using cDNA derived from LX-2 and a primer set listed in Table 1. The obtained DNA

fragments (497 bp) were inserted into a pmirGLO Vector (Promega, San Luis Obispo, CA, USA). LX-2 cells, plated in 96-well plates at a density of 2×10^4 cells/well 24 h prior to experiment, were transfected with 200 ng of reporter plasmid and miRNA precursor using Lipofectamine 2000. After 24 h, the medium was changed to 20 μl of PBS. The Dual-Glo Luciferase Assay System (Promega) was used to analyze luciferase expression in accordance with the manufacturer's protocol. Firefly luciferase activity was normalized to *Renilla* luciferase activity to adjust for variations in transfection efficiency among experiments.

Statistical analysis. Data presented as graphs are the means ± S.D. of at least three independent experiments. Statistical analysis was performed using Student's t-test. $P < 0.05$ was considered significant.

Results

Reduction of miR-195 expression during activation of primary-cultured HSCs

It has been known that, when maintained in a plastic culture plate, freshly isolated primary-cultured HSCs undergo spontaneous activation and transformation into myofibroblastic cells that express α-SMA and produce fibrogenic mediators, such as type I collagen and transforming growth factor-β. In our preliminary experiments using primary-cultured mouse HSCs, we noticed that the cells drastically decreased the expression of miR-195 when they underwent spontaneous activation (unpublished observation). The present study confirmed this notion as shown in Fig. 1A. miR-195 expression level certainly decreased in activation process of primary-cultured mouse HSCs. In contrast, the expression levels of α-SMA and cyclin E1 mRNA increased (Fig.

1B). Accordingly, we considered that miR-195 plays a role as an antiproliferative and antiactivating miRNA in HSCs. As a matter of fact, there was a study showing that miR-16 family including miR-195 inhibits proliferation of lung cancer cells by silencing cyclins D1 and E1, and CDK6 (Liu et al., 2008). The result indicated by Fig. 1 and the cited study together drove us to explore the IFN's antiproliferative action on HSCs (Mallat et al., 1995; Shen et al., 2002), focusing on miR-195 and cell cycle-related genes.

Effects of IFN-α and -β on proliferation of HSCs

First, we investigated the effects of type I IFNs on the proliferation of LX-2 cells using a WST-1 assay. LX-2 cells in control culture continued to grow during the experimental period of 7 days (Fig. 1C). IFN-α and -β both, but the latter more actively, decreased cell proliferation time-dependently at a concentration of 1,000 IU/ml, supporting the previous studies (Mallat et al., 1995; Shen et al., 2002). Dose-dependency of the growth inhibition is shown in IFN concentrations from 10 to 1,000 IU/ml (Fig. 1D).

Effects of IFN-α and -β on cell cycle distribution

To elucidate the mechanism of the growth inhibitory effect of IFN, we next examined the change in cell cycle distribution in response to IFN-α and -β treatment by flow cytometry. LX-2 cells were synchronized in G0/G1 phase by serum starvation for 24 h. In non-treated cells (control), population in G0/G1 phase was reduced after serum exposure, which was accompanied by the increase of population in S phase. This cell cycle transition peaked at 24 h (Fig. 2, upper panel). In cells treated with IFN-α or -β, the G0/G1 phase population was larger and the S phase population was smaller than in the control cells at 15 h and 24 h. In addition, the accumulation of cells in early S phase

was observed at 32–48 h (Fig. 2, middle and lower panels). These delays in cell cycle shift were more potent in IFN-β-treated cells than in IFN-α-treated cells. It was concluded that type I IFN hampered HSC proliferation through a delay in the cell cycle at the transition from G1 to S phase and in the progression of S phase.

Regulation of cyclin E1 and p21 expression by IFN-β

IFN-β was chosen in the following experiments because of its more potent inhibition of cell cycle progression than IFN-α, as described above. The transition from G1 to S phase and the progression of S phase are known to be influenced by various regulators (Golias et al., 2004). Among them, we found that IFN-β significantly decreased cyclin E1 mRNA expression levels by 0.6 – 0.7-fold at 6 h and 24 h and increased p21 mRNA expression levels by 1.4 – 2.3-fold at 6h, 24h, 48 h, and 72 h in LX-2 cells (Fig. 3). The expression levels of CDK4 and CDK6 was also reduced by IFN-β at early phase with less extent. The others showed negligible change within 24 h although variable dynamics were seen thereafter; changes of cyclin D1, CDK2, and p27 expression at late phase were toward cell cycle promotion with currently unknown reason.

Regulation of miR-195 expression by IFN-β

The result indicated from Fig. 1 strongly suggested the possibility that IFN-β increase the expression of miR-195 in LX-2 cells. To test this possibility, we examined the expression levels of miR-195 in IFN-β-treated LX-2 cells. As a result, the miR-195 expression level was significantly increased by IFN-β treatment at 24 h, 48 h and 72 h (Fig. 4A).

Regulation of cyclin E1 and p21 expression by miR-195

The results obtained from experiments shown in Fig. 3 and Fig. 4A led us to

hypothesize that IFN-β up-regulates the expression of miR-195, which then down-regulates the expression of cyclin E1 and up-regulates the expression of p21. In addition, there had been a study reporting that miR-195 targets E2F3, CDK6, and cyclin D1 in addition to cyclin E1 (Xu et al., 2009). Under these considerations, we examined the changes in the expression levels of the above-mentioned cell cycle-related molecules and CDK4 by introducing miR-195 precursor into LX-2 cells. Transfection of miR-195 precursor increased the miR-195 expression levels in LX-2 cells by up to 10,000–30,000 times compared with those in cells transfected with negative control (data not shown). Cyclin E1 mRNA and protein expression levels showed a remarkable reduction up to 72 h as result of miR-195 overexpression (Fig. 4B, C). On the other hand, p21 mRNA and protein expression levels showed a marked increase. CDK4, CDK6, and cyclin D1 expression levels were significantly changed at the mRNA level, but negligibly at the protein level. E2F3 mRNA and protein expression levels were unchanged (Fig. 4B, C). These results suggested that miR-195 mainly regulated cyclin E1 and p21 expression in LX-2 cells. Moreover, transfection of miR-195 precursor (50 nM) decreased the proliferation of LX-2 cells in the WST-1 assay (Fig. 4D). These results showed that miR-195 down-regulates endogenous cyclin E1 expression and up-regulates p21 expression, resulting in the attenuation of cell cycle progression and cell proliferation.

Interaction of miR-195 with cyclin E1 3'UTR in LX-2 cells

Next, we examined whether miR-195 interacted directly with cyclin E1 3'UTR in LX-2 cells. The predicted miRNA target sites for miR-195 in the cyclin E1 3'UTR were analyzed using TargetScan Human Release 5.1 (http://www.targetscan.org/). The cyclin